The Dispersion Behavior of Clay Particles in Poly(L-lactide)/Organo-Modified Montmorillonite Hybrid Systems

Pham Hoai Nam, Atsuhiro Fujimori, Toru Masuko

Department of Polymer Science and Engineering, Faculty of Engineering, Yamagata University, Johnan 4–3-16, Yonezawa, Yamagata, 992-8510, Japan

Received 21 January 2004; accepted 22 April 2004
DOI 10.1002/app.20899
Published online in Wiley InterScience (www.interscience.wiley.com).

ABSTRACT: Hybrids of poly(L-lactide)/organoclay (PLACHs) have been prepared via a melt-compounding process using poly(L-lactide) (PLLA) and three types of surface-treated montmorillonite modified with ammonium salts (M1, trimethyl octadecyl-; M2, dimethyl dioctadecyl-, and M3, bis(4-hydroxy butyl) methyl octadecyl-ammonium). The dispersed state of the clay particles in the PLLA matrix was examined by use of wide-angle X-ray diffraction, transmission electron microscopy, and polarizing optical microscopy. On melt-compounding PLLA and two organoclays (M1, M2) modified with the surfactants both carrying homogenous alkyl chains, we obtained intercalated hybrids with relatively uniform dispersion of nanometer-sized clay particles. On the other hand, the organoclay (M3) modified with a surfactant carrying alkyl chains end-capped with hydroxyl groups yielded the composite with flocculated particles. The flocculation of the particles originates from the hydrogen bonding among the hydroxyl groups of the component surfactant, those of the clay edge and those of both ends of PLLA chains. © 2004 Wiley Periodicals, Inc. J Appl Polym Sci 93: 2711–2720, 2004

Key words: poly(L-lactide); organoclay; morphology; WAXS; hybrid

INTRODUCTION

In recent years, polymer/clay composites (polymer/clay hybrids, abbreviated to PCHs) have attracted much attention as a new class of polymer-based composites, offering high potentials for ever-expanding versatile application.[1–4] The term PCH represents a composite composed of a matrix polymer coupled with a small percentage of clay minerals of nanometer thickness and several micrometers in size. Compared with conventional composites that contain fillers of millimeter or micrometer size, the loading of exfoliated layered clay imparts excellent properties to the matrix, such as high dimensional stability, gas barrier performance, high heat deflection temperature, and flame retardancy in addition to reinforced mechanical properties.[5–8]

So far, many different combinations of clays and matrix polymers for developing PCHs have been reported.[5–17] The first successful example was nylon-6/clay hybrid (NCH) developed by Usuki et al.[5–7] at Toyota Central Research and Development Laboratories. The matrix polymer was later extended to include some thermosetting resins, such as epoxy[9] and polyurethanes,[10] and also general purpose thermoplastics, such as polypropylene.[14,15] Usually, the clay of layered silicate, such as montmorillonites or smectites, is utilized in compounding and is converted in advance to so-called *organoclay* by replacing inorganic cations with quarternized ammonium salt to enhance their affinity toward the matrix polymer.[5–17]

The well-known technologies for PCH production are broadly classified as *intercalative polymerization and as direct blending* or *melt compounding* of clay into a polymer matrix.[1,3] The former consists of first dispersing organoclay particles in a monomer liquid from which some monomer molecules may be absorbed (intercalated) into the clay galleries and of subsequent polymerization of the monomer under suitable conditions.[5] The latter is compounding of an organoclay into a polymer matrix from either solution[18–20] or melt.[21] Vaia et al.[22] have reported the kinetics of polymer melt intercalation for polystyrene/clay hybrid system.

To improve the performance and properties of PCHs, a uniformly exfoliated clay structure obtained in the matrix is necessary. However, this process so far has encountered difficulties because of the quite weak clay–polymer interaction against the hindrance of electrostatic clay–clay attraction. To achieve a good dispersion and/or delamination of clay, there are at least two controlling factors: One is due to the chemical nature, such as high clay–polymer interaction,[7] and the other, the processing condition, such as high-shear melt-mixing.[23] The improvement of the interac-

Correspondence to: T. Masuko (tmasuko@yz.yamagata-u.ac.jp).

TABLE I
Characteristic Parameters for Natural Clay and Modified Clays

Sample	Clay	Ammonium salt	Organic content (w/o)	CEC_a[a] (mEq/100 *g*)
M0	Natural clay	—	—	—
M1	Modified clay	Trimethyl octadecyl	25.6	81.90
M2	Modified clay	Dimethyl dioctadecyl	41.4	75.22
M3	Modified clay	Bis(4-hydroxy butyl) methyl octadecyl	37.1	86.59

[a] Apparent cation exchange degree calculated from TG/DTA results.

tion between naturally hydrophilic clay and usually more or less hydrophobic polymer can be quite effectively achieved by hydrophobic modification of the clay with a suitable alkyl-ammonium surfactant and/or direct hydrophilic modification of the polymer by introducing more highly polar groups. Although such PCHs certainly have high potential for versatile future applications, there are serious drawbacks due to their environmental incompatibility arising from their matrix polymers. The blending or hybridization with clay minerals makes them more difficult to handle, yielding undegradable PCH waste.

A possible remedy to avoid such hazards is to replace the environmentally incompatible polymer matrix with a biodegradable one. In this context, a promising candidate is poly(L-lactide) (PLLA), which is obtained from renewable resources such as corn syrup, whey, dextrose, and cane and beet sugar. The PLLA is both a biodegradable and a biocompatible crystalline polymer with resultant environmental advantages over other synthetic polymers such as polypropylene and acts as a so-called *green* polymeric material to keep civilian life from the *undegradable* waste problem. Nowadays, PLLA are utilized for surgical implant materials, drug delivery systems, and film application.[24–26] The PLLA polymer offers high mechanical properties, thermal plasticity, and fabric ability as well as biocompatibility,[24,26] but it is still inferior in thermal stability. In fact, Pluta et al.[27] have reported the remarkably improved thermal stability in PLLA/clay hybrid systems compared with neat PLLA due to the uniform dispersion of clay particles in nanometer scale.

Accordingly, we attempted to explore the possibility of innovating environmentally friendly PLLA/clay hybrids (PLACHs) with excellent properties. There are already four reports available on the preparation and mechanical properties of PLLA/clay hybrids: Two were obtained by Ogata et al.[18] and Chang et al.[20] through solvent-casting and the other two were obtained by Pluta et al.[27] and Ray et al.[28] through melt-compounding. Although the structural models they proposed were somewhat different from each other, their PLACHs exhibited fairly good improvement in their mechanical properties.

To understand the details we thus examined the dispersion behavior of clay particles in PLLA/organo-modified montmorillonite hybrids. A problem was how to design and control the dispersion state of layered silicates in PLLA matrix. Poly(L-lactide) is known to exhibit crystalline polymorphism between an *orthorhombic* α-form[29] and a *pseudo-orthorhombic* β-form.[30] Another *orthorhombic* γ-form is also suggested in a recent report.[31] Such crystallization behavior of PLLA should influence the delamination of organoclay through clay–polymer interaction and vice versa. At first, we describe a simple melt-compounding of PLLA with Na^+-montmorillonite and its derivative modified with three different types of alkyl surfactants. The three alkyl surfactants employed are (1) trimethyl octadecyl-, (2) dimethyl dioctadecyl-, and (3) bis(4-hydroxy butyl) methyl octadecyl-ammonium salts. These surfactants, respectively, carry one long alkyl chain, two long alkyl chains, and one long alkyl chain having two alkyl chains with hydroxyl end-groups. Among

TABLE II
Characteristic Parameters of PLLA and Various PLLA/Clay Composites

Sample	Component	Inorganic content (%)	M_w ($\times 10^{-3}$ g · mol^{-1})	M_w/M_n	T_g[a] (°C)	T_m (°C)	χC[a,b](%)
PLLA	PLLA	—	159	1.86	59.9	168.6	22.5
S0	PLLA + M0	3.5	155	1.81	59.4	168.5	22.0
S1	PLLA + M1	3.6	164	2.04	60.1	169.1	24.0
S2	PLLA + M2	3.5	154	1.84	59.2	168.7	24.4
S3	PLLA + M3	3.5	160	1.86	61.0	169.0	21.0

[a] Results obtained by DSC measurement.
[b] χ_C, degree of crystallinity.

these three surfactants, we expected to find one leading to better clay delamination and finer dispersion of clay particles. Hopefully they might be effective due to the higher density of long alkyl chains in (2) or the higher polarity of alkyl chains in (3) compared to (1).

In this study, the dispersed clay structure is characterized by use of wide-angle X-ray diffraction (WAXD), transmission electron microscopy (TEM), and polarizing optical microscopy (POM). The preliminary information on PLLA crystallite morphology of PLACHs obtained by WAXD is also reported.

EXPERIMENTAL

Materials

The polymer used in this study was a high L-content (> 99%) commercial grade PLLA (Unitika Co. Ltd.), which was dried under vacuum at 100°C for 2 days and kept at room temperature in a silica gel-dried diskette for later use. Molecular characterization was carried out on a gel permeation chromatograph (GPC: JASCO 860-CO GPC/HPLC) using tetrahydrofuran (THF) carrier at 40°C with a flow rate of 1 mL/min and polystyrene (PS) elution standard. The results were (PS-reduced) weight-average molecular weight (M_w) = 20×10^4, number-average molecular weight (M_n) = 10×10^4, and the polydispersity index (M_w/M_n) was 1.94.

The clay samples were a purified Na^+-montmorillonite with the layer diameter size in the range 0.2 ~ 2.0 μm (trade name Kunipia-F) coded as M0, and its modified derivatives, all of which were supplied by Kunimine Co. The cation-exchange capacity (CEC) of M0 was 108.6 mEq/100 g. M0 was modified via a cation-exchange reaction with trimethyl octadecyl- or dimethyl dioctadecyl- or bis(4-hydroxy butyl) methyl octadecyl-ammonium salts, and coded, respectively, as M1, M2, and M3. According to the supplier, the organoclays were prepared using the following procedure: 15.2 g of M0 was suspended in 1,000 mL of warm water (about 70°C). A warm aqueous solution (about 80°C) of 16.6 mmol ammonium chloride salt was added gradually. After stirring for 1 h at ambient temperature, the exchanged clay was filtered and washed several times with water and then dried at 60°C to yield the organoclays. The organic content in the organoclays and the apparent cation exchange degree (CEC_a) of clay determined by thermogravimetric analysis (TGA: Seiko 5200 TG/DTA) are summarized in Table I. All these clay samples were dried under vacuum at 100°C for 2 days and subjected to the characterization and melt-compounding with neat PLLA.

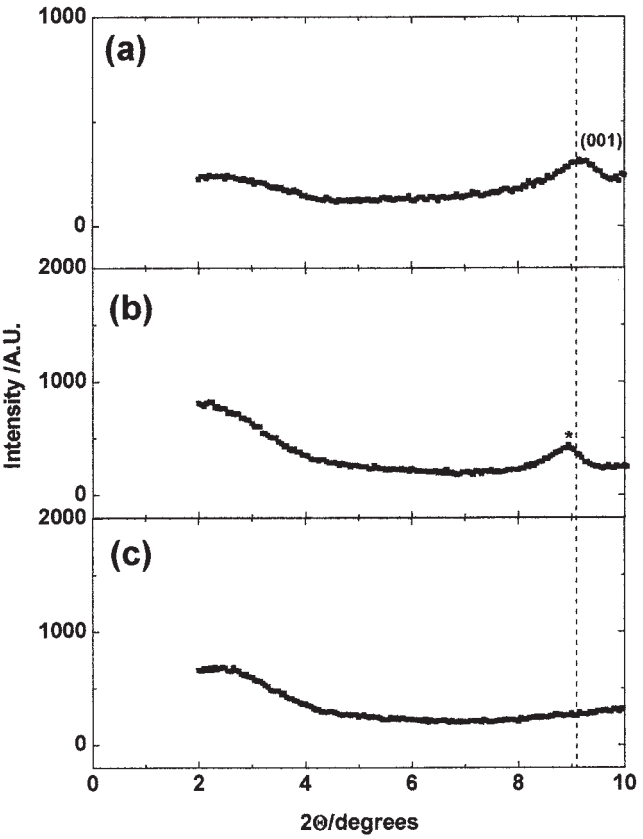

Figure 1 WAXD traces for (a) M0, (b) S0, and (c) PLLA. The dashed lines indicate the location of silicate (001) reflection of M0. The asterisks indicate a small peak for S0.

Hybrid preparation

The hybrids were prepared with an intensive mixer (counter-rotating mixer, Labo Plastomill, Model 30C150, Toyoseiki, Japan) by mechanical kneading at 190°C for 20 min with the rotor speed of 30 rpm. The torque was monitored during the mixing process to ensure thorough mixing of the compound. For comparison, native Na^+-montmorillonite was also mixed with neat PLLA in the same way to obtain a controlled sample. The corresponding composites were coded as S0 (PLLA + M0), S1 (PLLA + M1), S2 (PLLA + M2), and S3 (PLLA + M3). The inorganic content of each composite was analyzed by TGA under an N_2 purge and calculated from the residue left at 550°C. For each case, the TGA experiments were repeated at least twice. After melt-compounding, the collected molten materials were compression-molded into a 1-mm-thick sheet between polyimide films (Kapton® HN, Toray-Du Pont Co.) with a laboratory hot press at 190°C applying ~ 1 MPa pressure for 3 min. The molded specimens were quenched between two steel plates and then annealed in an air-bath at 115°C for 1 h to allow the specimens to be fully crystallized before subjecting them to all the measurements.

Characterization methods

Thermal analysis

The glass transition temperature (T_g), the melting temperature (T_m), and the degree of crystallinity (χ_c) of neat PLLA and the composite samples were determined using a DSC (Perkin–Elmer DSC Pyris 1). The instrument was calibrated with indium before the measurements. In each DSC run, a ~ 5-mg sample was heated under N_2 atmosphere from 25 up to 220°C at a heating rate of 10°C/min. For the estimation of χ_c from the heat of melting of each sample, we employed the value of 135 J/g for the melting enthalpy of 100% crystalline PLLA.[29] The results are summarized in Table II.

Gel permeation chromatography

Molecular characteristics of PLLA in as-prepared composites were characterized by using GPC in terms of M_w, M_n, and M_w/M_n. For the GPC test, each composite was dissolved in THF to make approximately 0.5% solution, followed by filtering through a 200-nm-pore-size filter to remove completely the clay from the solution. The results are also listed in Table II. The GPC results show that M_w of PLLA in the composites is smaller by approximately 20% than as-received neat PLLA. The melt-compounding with intensive mixing appears to have induced degradation of PLLA, especially more severely for S1, S2, and S3 than for S0 and neat PLLA. The decreased molecular weight of PLLA after melt-compounding may be explained due either to the shear mixing of PLLA and clay or to the presence of ammonium salts, which can promote hydrolysis of PLLA chains at the elevated temperature.

Wide-angle X-ray diffraction (WAXD)

The structural characteristics of the clay particles dispersed in the composite samples were characterized with a RAD-rA diffractometer (RIGAKU Co.). In a Θ–2Θ mode, a Ni-filtered CuKα radiation (wavelength, λ = 0.154 nm) was generated at 40 kV and 100 mA. The samples were scanned by using a step-scanning method with the step-width of 0.05° and 4-s intervals for the diffraction angle 2Θ in the range 2–35°. The diffracted X-ray beam was monochromatized by a pyrographite monochromatic system and monitored by a scintillation counter.

Transmission electron microscopy (TEM) and polarizing optical microscopy (POM)

To clarify the dispersion and the size of clay particles (or aggregates) in PLLA matrix, we used a TEM (Philips, CM-300) operated at an accelerating voltage of 200 kV. In the TEM observation, thin layers of around 70-nm thick were cut from the samples at room temperature using a Reichert ultramicrotome equipped with a diamond knife. No shadowing was conducted for these samples. A POM (Olympus, BH-2) equipped with a Linkam hot-stage (THM-600) was also used to observe the clay dispersion in the molten matrix. In this experiment, the samples were 30-μm thick, and their matrix PLLA was completely melted at 200°C for 10 min on the hot-stage before the observation.

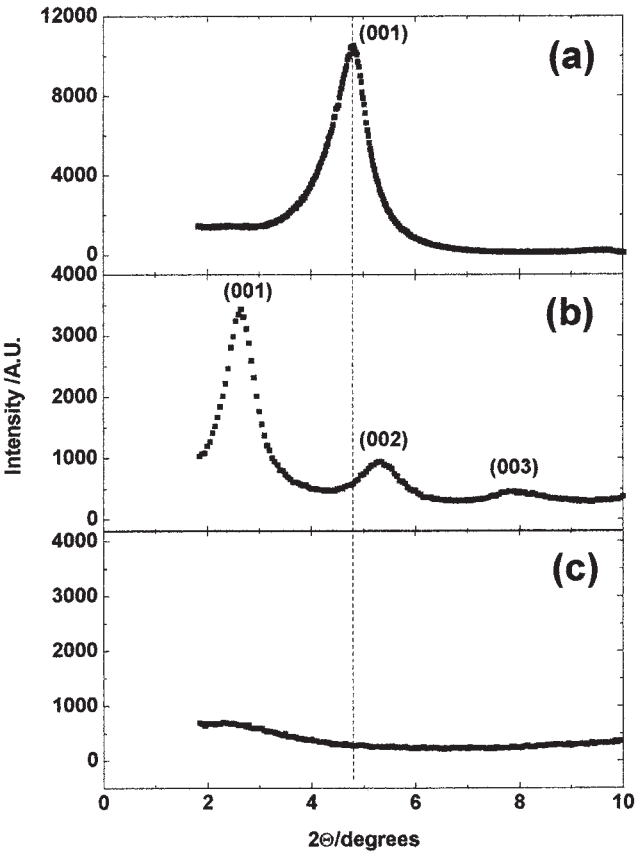

Figure 2 WAXD traces for (a) M1, (b) S1, and (c) PLLA. The dashed lines indicate the location of silicate (001) reflection of M1.

RESULTS AND DISCUSSION

X-ray diffraction of clay

Figures 1, 2, 3, and 4, respectively, show the XRD traces in the range of 2Θ = 2–10° for the natural clay contained in S0 and for three modified clays in S1, S2, and S3. The trace of neat PLLA is also displayed in each figure for contrasting the diffraction profiles of dispersed clay particles in the composites. From these WAXD profiles we calculated the d_{001} spacings and the results are summarized in Table III.

In Figure 1, we find that the mean interlayer spacing of the (001) plane (d_{001}) for the natural clay (M0) is 0.97 nm (2Θ = 9.15°), which can be compared with the

reference value.[32] On melt-compounding with neat PLLA to form S0, the peak still remains almost at the same position (d_{001} = 0.99 nm). The shape of the diffraction peak also appears to be unaffected by melt-compounding with PLLA. These results suggest that no change of internal clay structure occurred in this composite S0. The weak interaction between PLLA chains and hydrophilic M0 accompanied with its low and constant interlayer spacing, as revealed by the unchanged WAXD profile of M0, both imply that the clay particles are almost impossible to disperse thoroughly into the matrix.[3]

On the other hand, we find in Figures 2–4 for the organoclays that the (001) peak position significantly shifts toward the lower diffraction angle and the spacing (d_{001}) is doubled or even tripled, depending on the type of the surfactant. After melt-compounding these organoclays with PLLA, the (001) peak further shifts from 2Θ = 4.80° (d_{001} = 1.84 nm) to 2Θ = 2.65° (= 3.33 nm) for S1, from 2Θ = 2.75° (= 3.21 nm) to 2Θ = 2.30° (= 3.84 nm) for S2, and from 2Θ = 3.45° (= 2.56 nm) to 2Θ = 2.50° (= 3.53 nm) for S3. These expansions in d_{001} of the three kinds of organoclays suggest that the intercalation of PLLA chains into silicate gallery has taken place in these organoclay composites, indicating the effectiveness of the clay modifiers in reducing the surface energy of the clay and thus in promoting the polymer chain penetration into clay gallery. Since the increase in d_{001} is significantly less than root-mean-square end-to-end distance for a freely jointed random coil of PLLA chains (≅ 7.04 nm)[30,33] and the length of alkylammonium cations in clay (≅ 2.8 nm),[9,34] the configuration of the confined chain must be much more planar than that of the bulk random coil.

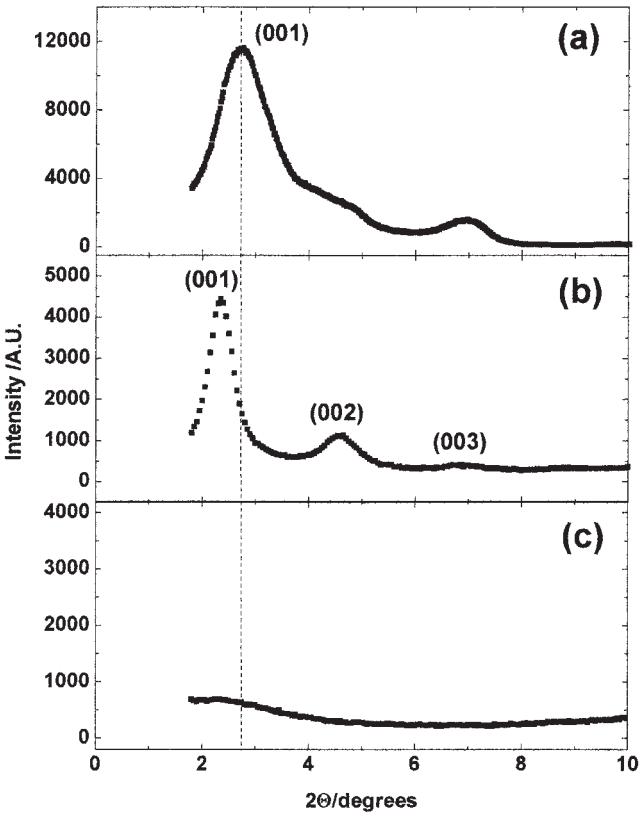

Figure 3 WAXD traces for (a) M2, (b) S2, and (c) PLLA. The dashed lines indicate the location of silicate (001) reflection of M2.

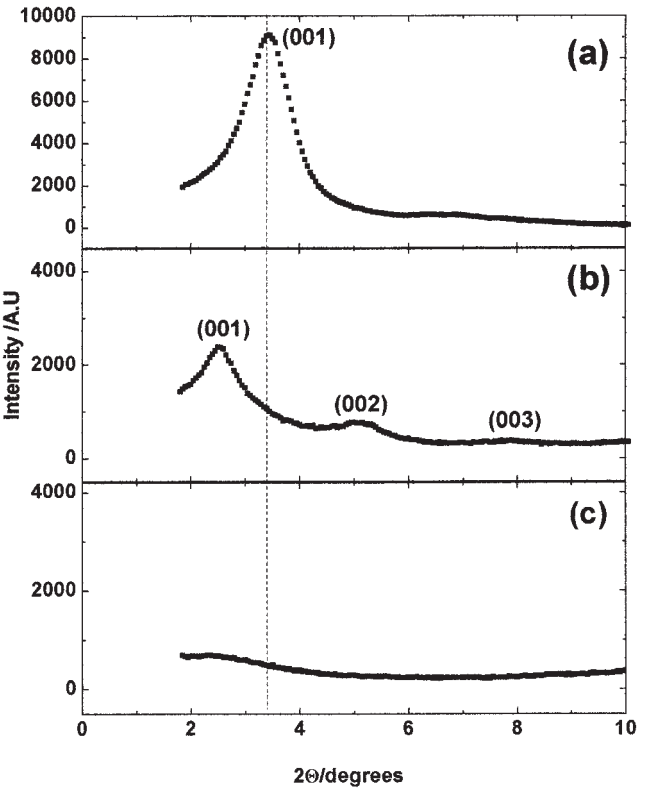

Figure 4 WAXD traces for (a) M3, (b) S3, and (c) PLLA. The dashed lines indicate the location of silicate (001) reflection of M3.

Besides the shifting of the sharp (001) diffraction peaks for the organoclays in the composites, we observe strong (002) and remnant (003) diffraction peaks. The results imply that clay particles still keep a highly ordered structure in the PLLA matrix even after extensive melt-compounding. Compared to clay particles in S1 and S2, the dispersed clay in S3 exhibits a less-ordered structure due to its relatively broader and weaker Bragg diffraction peaks. In such composites, the silicate layers have not been completely exfoliated, but several layers are stacked to form such an ordered structure of the clay particles.

The crystallite size normal to the (001) plane of the dispersed clay in PLLA matrix was calculated with the Scherrer equation.[35] The Scherrer equation applied is written as

$$h_{001} = \frac{K\lambda}{\beta \cos\Theta_{001}} \quad (1)$$

TABLE III
Structural Parameters of Natural Clay, Modified Clay, and Various PLLA/Clay Composites

Sample	d_{001}[a)] (nm)	h_{001}[a)] (nm)	h_M[a)] (nm)	L_M[a)] (μm)	L^*_M[a)] (μM)	d_M[a)] (μm)	d^*_M[a)] (μm)
M0	0.97	7.9	—	0.2 ≈ 2.0[b)]			—
M1	1.84	11.6	—	0.2 ≈ 2.0[b)]			—
M2	3.21	7.2	—	0.2 ≈ 2.0[b)]			—
M3	2.56	9.0	—	0.2 ≈ 2.0[b)]			—
S0	0.99	13.2	—		118.7 ± 28.3		108.9 ± 31.4
S1	3.33	13.1	12.0 ± 2.0	0.5 ± 0.2		0.2 ± 0.1	
S2	3.84	16.3	14.3 ± 2.4	0.7 ± 0.4		0.2 ± 0.2	
S3	3.53	11.0	5.3 ± 1.7		59.9 ± 26.6		158.1 ± 104.8

[a] d_{001}, the (001) interlayer spacing of clay calculated from WAXD results; h_{001}; the dispersed clay thickness calculated by using the Scherrer equation; h_M, L_M, and d_M: the thickness, length, and correlation length, respectively, of dispersed clay calculated by TEM observations; L^*_M and d^*_M: the length and correlation length, respectively, of the clay aggregates measured by POM observations;
[b] Measured by atomic force microscopy.[37]

where K is a constant (= 0.91), λ is the X-ray wavelength (= 0.154 nm), β is the width of the Bragg diffraction peak determined by the full width at half maximum in radian units, and Θ_{001} is the diffraction peak position of (001) plane. The calculated crystallite size (h_{001}), i.e., the thickness of the dispersed clay in PLLA matrix, is summarized in Table III. These h_{001} of dispersed clay in PLLA matrix for all materials are calculated to be less than 15 nm. After composite preparation, the natural clay in S0 increases h_{001} with the constant d_{001}, implying that a strong aggregation of clay particles has taken in the composite. On the other hand, h_{001} of the dispersed clays in S1, S2, and S3 increase with d_{001}. The detailed study on the numbers of individual layers stacked in clay for these samples will be described later by TEM results.

Microscopic observation of clay hybrids

Figure 5 shows the POM micrographs for (a) S0, (b) S1, (c) S2, and (d) S3 in the molten state at 200°C. Dispersed clay aggregates are shown as the bright areas

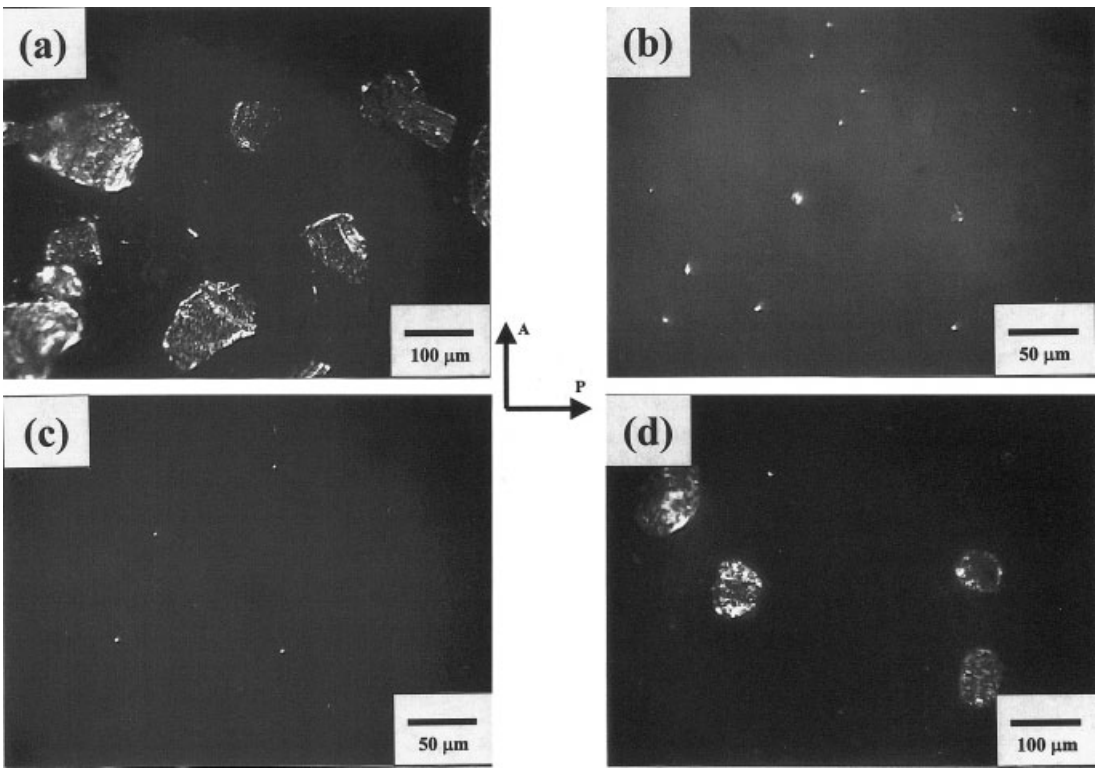

Figure 5 POM micrographs showing for: (a) S0, (b) S1, (c) S2, and (d) S3 in the molten state. The bright areas indicate the existence of clay particles, and the dark areas indicate the molten PLLA matrix.

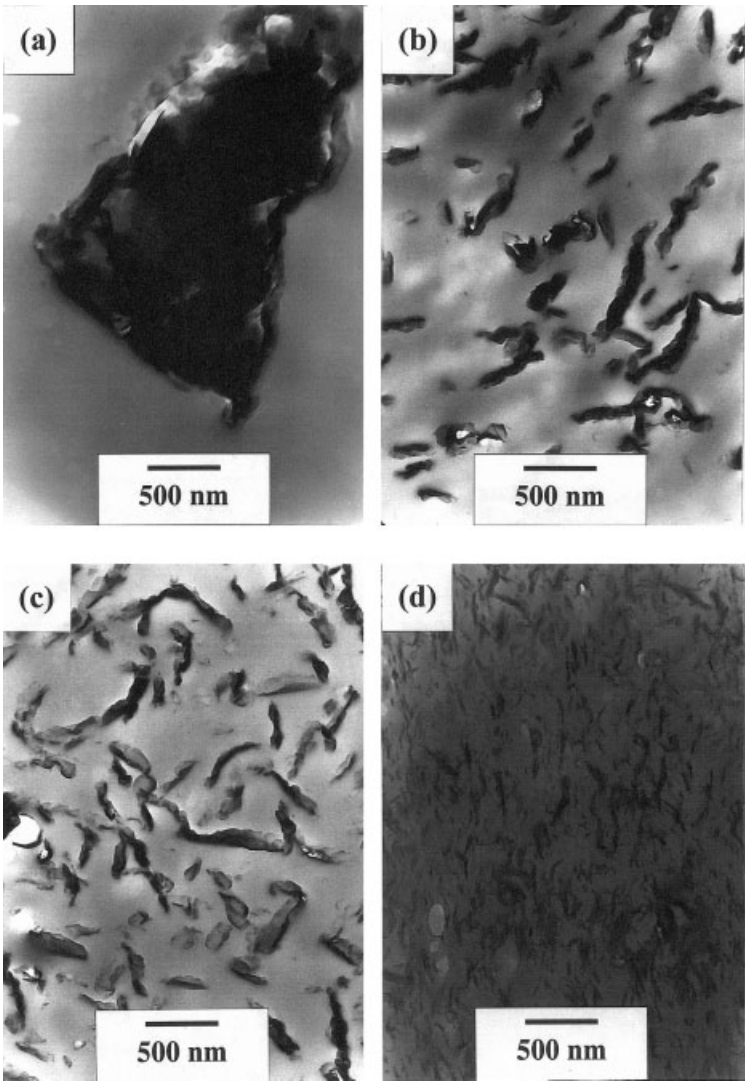

Figure 6 TEM micrographs for (a) S0, (b) S1, (c) S2, and (d) S3. The dark areas are the partly rolled shapes or a part of the cross section of silicate layers and the bright areas are the PLLA matrix.

in the dark background of the PLLA matrix. From these photographs the average sizes of the clay aggregates, L_M^*, can be estimated and are listed in Table III. Figure 5(a) shows that the natural clay particles with the size of 0.2 $\sim$ 2.0 μm are aggregated in S0 in the form of tactoids of the size L_M^* as large as $\sim$ 118.7 $\pm$ 28.3 μm. Obviously, the clay particles (or platelets) in S0 underwent stacking and a large-scale three-dimensional aggregation during melt-compounding. Interestingly, we see in Figure 5(b) (S1) and Figure 5(c) (S2) the much smaller clay platelets of micron-size are rather uniformly dispersed (their precise sizes will be statistically calculated via TEM observation later). On the other hand, Figure 5(d) for S3 shows a few aggregates with a fairly large size of $L_M^* \approx 59.9 \pm 26.4 \mu m$.

The nanoscale structure of the dispersed clay particles in the PLLA matrix is clearly shown by TEM micrographs. Figure 6 shows the typical TEM images for (a) S0, (b) S1, (c) S2, and (d) S3. In Figure 6(a), we see the aggregation structure of clay in S0. The clay particles densely accumulate and exist in a manner as a separate phase to the matrix, indicating strong incompatibility between the clay and the polymer. Interestingly, for S1 [Fig. 6(b)] and S2 [Fig. 6(c)], we observe the uniform dispersion of clay particles in the polymer matrix where most of the clay particles show their partly rolled shapes or a part of their cross section perpendicular to the sample surface. On the other hand, Figure 6(d) shows the flocculation structure of clay particles for S3 where some of the dispersed clay particles meet each other via their edges, and the others still thoroughly disperse in the matrix. Such an arrangement of clay particles thus forms an open flocculation structure of clay in S3.[36] This type of flocculation is probably due to the formation of hydrogen bonding among the hydroxyl groups of the component surfactant, those of clay edge and those of both ends of the PLLA chains. We have already confirmed

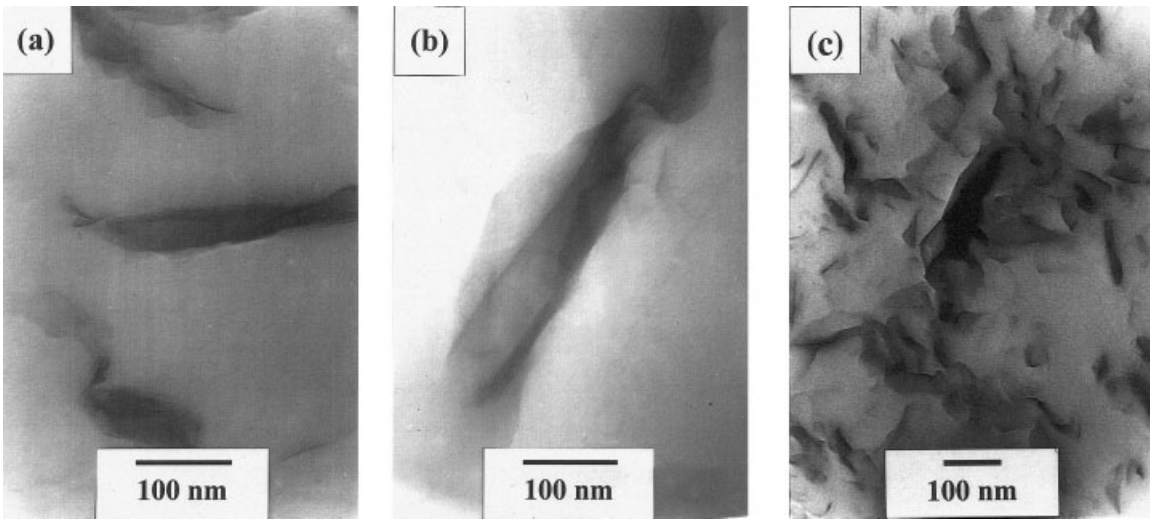

Figure 7 High-magnification TEM micrographs for (a) S1, (b) S2, and (c) S3.

this result by using infrared spectroscopy (IR) and it has been reported elsewhere.[37]

Figure 7 shows the typical TEM images at high magnification for (a) S1, (b) S2, and (c) S3. From these TEM observations, we find five to seven individual layers stacked in each dispersed clay particles for S1 and S2, but only one to three individual layers for S3. The relatively stronger interaction between PLLA chain and hydroxylated ammonium surfactant of clay in S3 probably results in the thinner clay particles contained within the flocculation structure.

The finding from TEM is actually consistent with the above WAXD results for the ordered structure of dispersed clay in PLACHs. From the TEM results, we statistically calculated the form variables for clay particles, i.e., the thickness (h_M), the length (L_M), and the correlation length (the distance between the middle points of two neighboring clays) (d_M) in Table III. Each

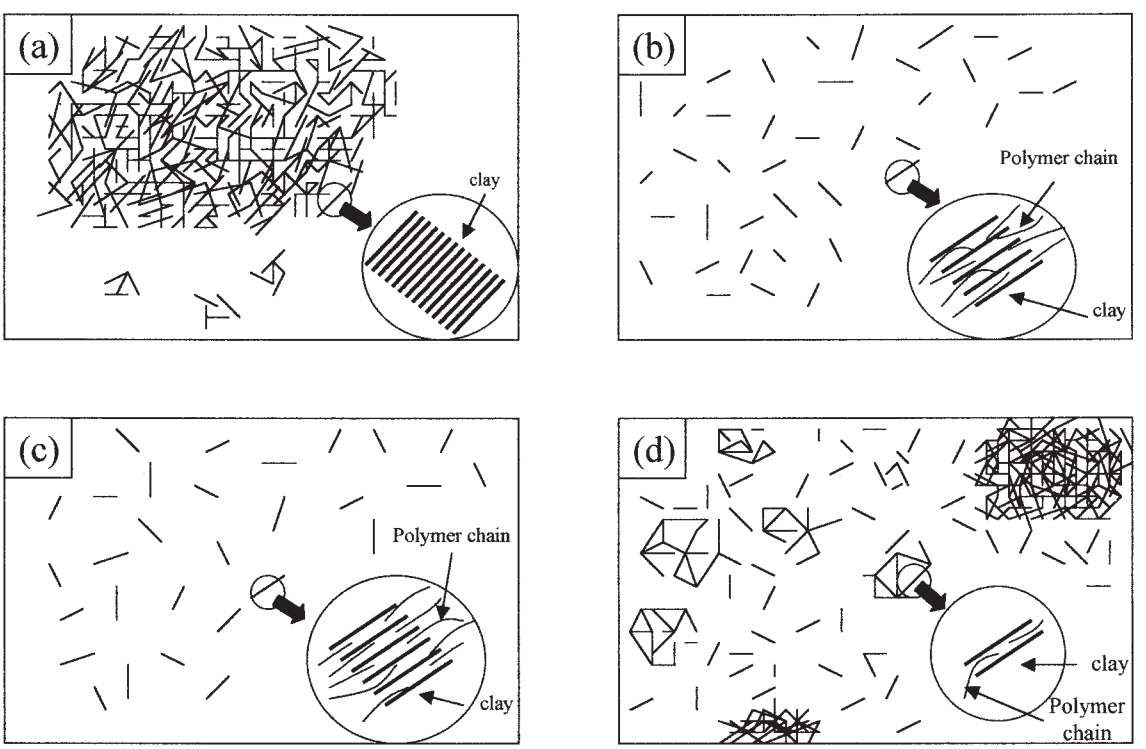

Figure 8 Clay dispersion structure in PLLA matrix for (a) S0, (b) S1, (c) S2, and (d) S3.

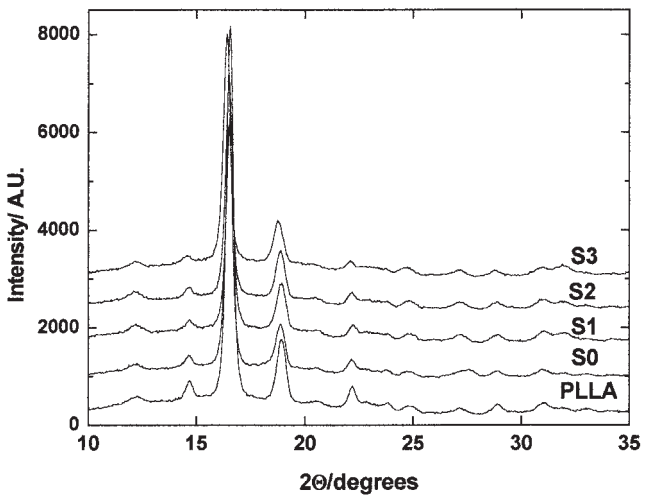

Figure 9 WAXD traces for PLLA and its composites in the range of $2\Theta = 10–35°$. The diffraction curves are vertically offset for clarity.

form variable was calculated from more than 100 clay particles of 8 ~ 10 TEM pictures taken at various places in the sample. Table III indicates that h_M is comparable to the value of h_{001} calculated with the Scherrer equation. In addition, these values are in the same order of magnitude with the long period of the polymer crystallite, implying a possibility for the relationship between clay and PLLA crystallite in term of crystallization, which will be investigated in a separate paper. For S1 and S2, the value of d_M is almost half compared to that of L_M, suggesting that the densely packed structure of the dispersed clay particles is formed. This feature of clay particles thus possibly affects the mechanical properties of the resultant composites. For instance, the clay particles here can not rotate, but translate under shearing or elongation force in molten state. From the POM and TEM observations, the illustration of the dispersed clay structure is shown in Figure 8. Thus, PLLA/clay composites prepared by melt-compounding between PLLA and natural clay or clay modified with various alkyl ammoniums result in the composites having different dispersion structures of clay particles from nanometer to micrometer lengths.

Polymorphism of PLLA

Figure 9 shows the WAXD traces for PLLA and its composites in a range of 10 - 35°. These WAXD traces are almost identical with that of the L-lactide homopolymer.[38] All diffraction profiles suggest the formation of only the orthorhombic α-form for PLLA and its composites. The β-form, which is usually formed via a spinning or drawing process at high temperature, does not exist in the present study as evidenced by the absence of its typical (003) peak around $2\Theta = 30°$.[30,39] With the addition of clay in PLLA, all of the composites show no shift in diffraction peaks, implying that there is no significant effect of the clay particles on the crystal structure of the matrix PLLA.

The detailed study on the relationship between the mechanical properties and the hierarchical structure viewed from the nanoscale structure of clay dispersed within the interfibrillar space of PLLA crystallite to the microscale spherulitic texture of PLLA will be reported elsewhere.

CONCLUSION

In this study, we prepared PLLA/organo-modified montmorillonite hybrids via the melt-compounding process and investigated the dispersed characteristics of clay particles in the matrix. The results are as follows:

1. The combination of PLLA and natural clay resulted in an immiscible composite with strongly aggregated tactoids of clay dispersed in the PLLA matrix.
2. The organic modification of clay with the trimethyl octadecyl or dimethyl dioctadecyl ammonium salts results in the intercalated hybrids with the uniform dispersion of nanometer-sized clay particles in the PLLA matrix, while the bis(4-hydroxy butyl) methyl octadecyl ammonium salt lead to the composite with the flocculation of clay particles.

The authors highly appreciate the contributions of Mr. Kazuo Sasaki of Yamagata University, who carried out some parts of the WAXD work and Mr. Naoya Ninomiya for his help with various experiments.

References

1. LeBaron, P. C.; Wang, Z.; Pinnavaia, T. J. Appl Clay Sci 1999, 15, 11.
2. Vaia, R. A.; Price, G.; Ruth, P. N.; Nguyen, H. T. Lichtenhan, J. Appl Clay Sci 1999, 15, 67.
3. Alexandre, M.; Dubois, P. Mater Sci Eng 2000, 28, 1.
4. Manias, E.; Touny, A.; Wu, L.; Strawhecker, K.; Lu, B.; Chung, T. C. Chem Mater 2001, 13, 3516.
5. Usuki, A.; Kojima, Y.; Okada, A.; Fukushima, Y.; Kurauchi, T.; Kamigaito, O. J Mater Res 1993, 8, 1179.
6. Yano, K.; Usuki, A.; Okada, A.; Kurauchi, T.; Kamigaito, O. J Polym Sci, Polym Chem 1993, 31, 2493.
7. Kawasumi, M.; Hasegawa, N.; Kato, M.; Usuki, A.; Okada, A. Macromolecules 1997, 30, 6333.
8. Messersmith, P.; Giannelis, E. P. J Polym Sci, Polym Phys 1995, 33, 1047.
9. Lan, T.; Padmananda, D. K.; Pinnavaia, T. Chem Mater 1995, 7, 2144.
10. Agag, T.; Takeichi, T. Polymer 2000, 41, 7083.
11. Huang, J. C.; Zhu, Z.; Yin, J.; Qian, X.; Sun, Y. Polymer 2001, 42, 873.

12. Okamoto, M.; Morita, S.; Taguchi, H.; Kim, Y. H.; Kotaka, T.; Tateyama, H. Polymer 2001, 42, 1201.
13. Okamoto, M.; Morita, S.; Kotaka, T. Polymer 2001, 42, 2685.
14. Tien, Y.; Wei, K. H. Polymer 2001, 42, 3213.
15. Nam, P. H.; Maiti, P.; Okamoto, M.; Kotaka, T.; Hasegawa, N.; Usuki, A. Polymer 2001, 42, 9633.
16. Galgali, G.; Ramesh, C.; Lele, A. Macromolecules 2001, 34, 852.
17. Lepoittevin, B.; Devalckenare, M.; Pantoustier, N.; Alexandre, M.; Kubies, D.; Calberg, C.; Jerome, R.; Dubois, P. Polymer 2002, 43, 4017.
18. Ogata, N.; Jimenez, G.; Kawai, H.; Ogihara, T. J Polym Sci, Polym Phys 1997, 35, 389.
19. Lagaly, G. Appl Clay Sci 1999, 15, 1.
20. Chang, J. H.; An, Y. U.; Sur, G. S. J Polym Sci, Polym Phys 2003, 41, 94.
21. Vaia, R.; Ishii, H.; Giannelis, E. P. Chem Mater 1993, 5, 1694.
22. Vaia, R.; Jandt, K. D.; Kramer, E. J.; Giannelis, E. P. Macromolecules 1995, 28, 8080.
23. Dennis, H. R.; Hunter, D. L.; Chang, D.; Kim, S.; White, J. L.; Cho, J. W.; Paul, D. R. Polymer 2001, 42, 9513.
24. Datta, R.; Tsai, S. P.; Bonsignore, P.; Moon, S. H.; Frank, J. R. FEMS Microbiol Rev 1995, 16, 221.
25. Vert, M.; Schwarch, G.; Coudane J. JMS–Pure Appl Chem 1995, A32, 787.
26. Lunt, J. Polym Degrad Stab 1998, 59, 145.
27. Pluta, M.; Galeski, A.; Alexandre, M.; Paul, M. A.; Dubois, P. J Appl Polym Sci 2002, 86, 1497.
28. Ray, S. S.; Maiti, P.; Okamoto, M.; Yamada, K.; Ueda, K. Macromolecules 2002, 35, 3104.
29. Miyata, T.; Masuko, T. Polymer 1997, 38, 4003.
30. Hoogteen, W.; Postema, A. R.; Pennings, A. J.; TenBrinke, G.; Zugenmaier, P. Macromolecules 1990, 23, 634.
31. Cartier, L.; Okihara, T.; Ikada, Y.; Tsuji, H.; Puiggali, J.; Lotz, B. Polymer 2000, 41, 8909.
32. Fukushima, Y. Clays Clay Miner 1984, 4, 320.
33. Stroble, G. R. The Physics of Polymers; Springer-Verlag: New York, 1997; pp 20–28.
34. Kakegawa, N.; Ogawa, M. Appl Clay Sci 2002, 22, 137.
35. Cullity, B. D. Element of X-ray Diffraction; Addison-Wesley: Reading, MA, 1978; pp 99–106.
36. Olphen, H. V. An Introduction to Clay Colloid Chemistry; John Wiley: New York, 1977; p 97.
37. Nam, P. H.; Fujimori, A.; Masuko, T. e-Polymers, no. 005, 2004.
38. Ikada, Y.; Khosrow, J.; Tsuji, H.; Hyon, S. H. Macromolecules 1987, 20, 906.
39. Sawai, D.; Takahashi, K.; Imamura, T.; Nakamura, K.; Kanamoto, T.; Hyon, S. H. J Polym Sci, Polym Phys 2002, 40, 95.